NASA Neptune Data Analysis Program Grant NAGW-2742

PI: John Spencer

Final Technical Report

Extensive computer modeling of the migration of volatiles on Triton, particularly N_2, was performed under this grant. The PI also attended and actively participated in the Neptune/Triton conference in Tucson in January 1992. The results of the work are contained in the publication Spencer, J.R. and J.M. Moore (1992) *The Influence of Thermal Inertia on Temperatures and Frost Stability on Triton*, published in *Icarus*, **99**, 261-272. A reprint is enclosed. The following summary of the work and its conclusions is taken from the abstract of the paper.

Seasonal subsurface heat conduction can have a large influence on Triton's N_2 frost distribution. Increasing surface thermal inertia reduces the thickness and extent of seasonal N_2 frosts. If the thermal inertia of the non-volatile substrate is greater than about 30% of the value for nonporous H_2O or CO_2, or if nonporous H_2O or CO_2 are overlain by a porous regolith of low thermal inertia but less than a few meters thick, the northernmost latitudes visible to Voyager should have been frost-free at the time of the encounter, possibly accounting for their relatively low albedo. If the substrate in the northern hemisphere has sufficiently low albedo and/or emissivity and also has a thermal inertia comparable to nonporous H_2O or CO_2, there may be no seasonal or permanent N_2 deposits in the northern hemisphere at all. Because this model, like previous ones, predicts a monotonic recession of permanent N_2 deposits towards the poles and very limited seasonal N_2 frost in the southern hemisphere at Voyager time, and because of new spectroscopic evidence for non-volatile CO_2 on Triton's bright southern hemisphere, we consider it possible that much of the bright material on Triton's southern hemisphere is not N_2. Bright non-volatiles in the southern hemisphere may allow seasonal N_2 frosts to form there during the southern summer, possibly helping to explain Triton's spectroscopic changes during the past decade. All the models considered here predict tenfold or greater seasonal variations in atmospheric pressure, with pressure currently increasing in high thermal inertia models and decreasing in models with low thermal inertia.

ICARUS 99, 261–272 (1992)

The Influence of Thermal Inertia on Temperatures and Frost Stability on Triton

JOHN R. SPENCER

Lowell Observatory, 1400 W. Mars Hill Road, Flagstaff, Arizona 86001

AND

JEFFREY M. MOORE

NASA Ames Research Center, Space Science Division, MS 245-3, Moffett Field, California 94035

Received March 3, 1992; revised July 8, 1992

Seasonal subsurface heat conduction can have a large influence on Triton's N_2 frost distribution. Increasing surface thermal inertia reduces the thickness and extent of seasonal N_2 frosts. If the thermal inertia of the nonvolatile substrate is greater than about 30% of the value for nonporous H_2O or CO_2, or if nonporous H_2O or CO_2 is overlaid by a porous regolith of low thermal inertia but less than a few meters thick, the northernmost latitudes visible to Voyager should have been frost-free at the time of the encounter, possibly accounting for their relatively low albedo. If the substrate in the northern hemisphere has sufficiently low albedo and/or emissivity and also has a thermal inertia comparable to that of nonporous H_2O or CO_2, there may be no seasonal or permanent N_2 deposits in the northern hemisphere at all. Because this model, like previous ones, predicts a monotonic recession of permanent N_2 deposits toward the poles and very limited seasonal N_2 frost in the southern hemisphere at Voyager time, and because of new spectroscopic evidence for nonvolatile CO_2 on Triton's bright southern hemisphere, we consider it possible that much of the bright material on Triton's southern hemisphere is not N_2. Bright nonvolatiles in the southern hemisphere may allow seasonal N_2 frosts to form there during the southern summer, possibly helping to explain Triton's spectroscopic changes during the past decade. All the models considered here predict 10-fold or greater seasonal variations in atmospheric pressure, with pressure currently increasing in high-thermal-inertia models and decreasing in models with low thermal inertia.

I. INTRODUCTION

This paper attempts to shed light on Triton's atmospheric pressure and composition, and its surprising surface albedo patterns, by considering the influence of the subsurface seasonal heat flow on surface temperatures and frost stability. This factor has not been considered in previous published Triton models, but turns out to have a potentially large influence on the distribution of volatiles on Triton's surface.

I.A. Previous Work

The first detailed consideration of frost stability on Triton was by Trafton (1984), who noted that efficient atmospheric transport of latent heat between globally distributed frost patches was likely to equalize global frost temperatures regardless of local insolation. Though Trafton's pre-Voyager model considered CH_4 frost, Ingersoll (1990) showed that Voyager observations of Triton's albedo and atmospheric temperature and pressure (e.g., Broadfoot *et al.* 1989) indicated that Trafton's isothermal frost model was applicable to N_2 frost on Triton.

Spencer (1990) constructed a historical model to track long-term trends in N_2 frost migration, assuming zero surface thermal inertia, isothermal frost, and Triton's complex seasonal variations in subsolar latitude. The model demonstrated that permanent frost deposits should migrate monotonically to the poles (which are the points of minimum seasonally averaged insolation), and the global equivalent of tens of grams per square centimeter of seasonal deposits should migrate indefinitely between the hemispheres, forming extensive seasonal frost caps in the winter hemisphere. Because the southern hemisphere was experiencing summer at the time of the Voyager encounter, the model predicted the presence there of a relatively small remnant of the previous winter's seasonal cap and extensive frost-free regions. This prediction is in apparent contradiction with the observed brightness of the entire southern hemisphere (McEwen 1990). Simi-

Presented at Neptune/Triton Conference in Tucson, Arizona, during January 6–10, 1992.

0019-1035/92 $5.00

larly, the model predicted tens of grams per square centimeter of fresh seasonal frost extending down to the equator in the northern hemisphere, in apparent contradiction with the relative darkness of the visible northern hemisphere.

Spencer (1990) therefore suggested that fresh frost on Triton might be relatively dark, brightening with time due to insolation, in a manner similar to the Martian polar caps. The dark northern hemisphere seen by Voyager would then be covered by fresh, relatively low-albedo N_2 frost, while the southern hemisphere would contain a mixture of bright, nonvolatile substrate and older, brighter N_2 frost.

The model also predicted that the atmospheric pressure on Triton should be very unstable, varying by factors of 10 or more, because of the small mass of the atmosphere and its control by the vapor pressure of the surface frosts. Low emissivities, perhaps as low as 0.5, appeared to be necessary to explain the observed atmospheric pressure, given the high albedos derived photometrically from the Voyager data (McEwen 1990, Hillier *et al.* 1991).

Stansberry *et al.* (1990) looked in more detail at the albedo patterns seen by Voyager and determined the stability of surface frosts as a function of local albedo and latitude, again assuming instantaneous equilibrium with diurnally averaged sunlight. They reached similar conclusions about the likely current deposition of N_2 frost in the visible northern hemisphere and the apparent low emissivity of the N_2 frost.

Moore and Spencer (1990) suggested a permanent global asymmetry in the N_2 frost distribution on Triton: the Koyaanismuuyaw (Hopi for "moon out of balance") hypothesis. They suggested that the high albedo of the southern cap might keep it cold enough to be permanently stable, with the thin seasonal northern hemisphere frost remaining dark because it was so transparent that a dark, nonvolatile substrate was visible through it. The widespread presence of probable collapse features in the northern hemisphere led them to suggest that there has been a net nonreversible flux of surface volatiles from the northern to the southern hemisphere over much of the satellite's history.

While Spencer (1990) suggested that much of the bright southern hemisphere of Triton was nonvolatile substrate material with some remnant seasonal frost, Kirk and Brown (1991) offered the alternative that the bright region was largely a permanent cap of solid N_2. They suggested that the monotonic poleward shrinkage of the permanent cap predicted by Spencer (1990) was counteracted by viscous spreading of the cap. For instance, a stable cap extending 45° from the pole could thus be maintained if the cap was 1.7 km thick. Brown and Kirk (1991) also showed that internal geophysical heat flow was potentially important in controlling the surface N_2 distribution and might provide a positive feedback mechanism that could maintain an inhomogeneous N_2 frost distribution.

I.B. Problems to Be Addressed

The work presented here applies a thermophysical historical model to long-term and seasonal volatile migration on Triton. It demonstrates the potential importance of seasonal thermophysics and shows its influence on frost distribution. In particular, we attempt to address the question of the relative darkness of Triton's northern latitudes and the possibility of a permanent hemispheric asymmetry in the frost distribution.

II. POSSIBLE ROLE OF SEASONAL SUBSURFACE HEAT CONDUCTION

Seasonal surface temperature variations are moderated by the conduction of heat into the subsurface during the summer and its release during the winter. The ability of the surface to store heat is characterized by the thermal inertia, Γ, given by $\Gamma = \sqrt{k\rho c}$, where k is the thermal conductivity, ρ, is the density, and c is the specific heat. Seasonal heat storage is uniquely important on Triton and Pluto because of their low surface temperatures and the T^4 dependence of black body thermal radiation (Sykes *et al.* 1987, Spencer *et al.* 1989). The low temperature reduces the efficiency of radiative heat loss during the winter, so more of the heat stored in the subsurface during the previous summer is retained. As a result, temperatures far removed from equilibrium values are possible.

A second factor enhancing the effect of seasonal subsurface heat conduction on Triton is the deep penetration of the seasonal thermal wave into the subsurface, because of the long seasons. The penetration depth d is given by $d = \sqrt{kt_S/(2\pi\rho c)}$, where t_S is the seasonal timescale (one Neptune orbital period, 164 years), and thus for constant thermophysical properties will be nine times greater on Neptune than on Mars, for instance. The seasonal thermal wave will thus penetrate into deeper materials that are likely to be less porous and have higher thermal inertia than if the seasons were shorter (see Table I). Though long seasons per se allow temperatures to come closer to equilibrium values, the deep penetration of the thermal wave counteracts this effect if thermal inertia increases with depth.

III. LIKELY SUBSURFACE THERMOPHYSICAL STRUCTURE

III.A. Nonvolatile Substrate

The nonvolatile substrate on Triton, over which the frosts migrate, is likely to consist of H_2O, which is proba-

TABLE I
Thermophysical Properties of Relevant Ices

Ice	Temperature (K)	c (erg g^{-1} K^{-1})	k (erg cm^{-1} sec^{-1} K^{-1})	ρ (g cm^{-3})	Γ ($\sqrt{k\rho c}$) (erg cm^{-2} sec$^{-1/2}$ K^{-1})	Triton seasonal skindepth d ($\sqrt{kt_S/(2\pi\rho c)}$) (cm)
H_2O	30	2.3×10^6	2.0×10^6	0.93	2.1×10^6	28,000
H_2O	40	3.5×10^6	1.5×10^6	0.93	2.2×10^6	19,000
$N_2(\alpha)$	30	1.2×10^7	2.9×10^4	1.0	5.9×10^5	1,400
$N_2(\beta)$	40	1.3×10^7	2.1×10^4	1.0	5.3×10^5	1,100
CH_4	30	1.5×10^7	3.8×10^4	0.52	5.4×10^5	2,000
CH_4	40	1.8×10^7	4.2×10^4	0.52	6.3×10^5	1,800
CO_2	30	2.9×10^6	4.2×10^5	1.7	1.4×10^6	8,300
CO_2	40	4.5×10^6	2.7×10^5	1.7	1.4×10^6	5,400
Rhea regolith	~90	8.3×10^6	200	0.5	3×10^4	3[a]
Rhea regolith	40	3.5×10^6	600	0.5	3×10^4	500

Note. Ice thermal properties are from numerous sources compiled by Croft (manuscript in preparation). Seasonal timescale t_S used in calculating skindepths is 164 years, Neptune's orbital period. Latent heat of N_2 α/β phase transition = 8.17×10^7 erg g^{-1}. The Rhea regolith Γ at 90 K is derived observationally from the subsolar temperature of Rhea, and k(90 K) is derived from this, assuming $\rho = 0.5$ and the known c(90 K) for water ice. Regolith k is then assumed to have the same T dependence as nonporous ice, allowing an estimate of Γ and d for the Rhea regolith at Triton temperatures.

[a] Diurnal skindepth on Rhea.

bly abundant in Triton's interior though it has not been detected spectroscopically on its surface, or CH_4 or CO_2, which are seen in the reflectance spectrum. Table I gives the relevant thermophysical properties for H_2O, CH_4, CO_2, and N_2 ice at 30 and 40 K. Our model uses substrate thermal inertias up to 2×10^6 erg cm^{-2} sec$^{-1/2}$ K^{-1}, a good approximation for nonporous H_2O or CO_2 ices.

By analogy with other solid planetary surfaces, any nonporous substrate on Triton is liable to be overlain with a porous regolith of lower thermal inertia. Rhea, because of its icy surface, high albedo, and relatively low surface temperatures, is the closest analog to Triton for which we have thermophysical data. The thermal inertia of Rhea, as determined from a comparison of its albedo and subsolar temperature, is about 3×10^4 erg cm^{-2} sec$^{-1/2}$ K^{-1} (Spencer 1988, 1989), implying a conductivity of several hundred erg cm^{-1} sec^{-1} K^{-1} (Table I). Values for the icy Galilean satellites are similar. This value applies to the region within the diurnal skindepth d of Rhea's surface, i.e., the top few centimeters of the regolith. However, as discussed above, the deep penetration of Triton's diurnal thermal wave (several meters) is likely to produce higher effective thermal inertias.

Unlike on Rhea, heat conduction in a porous regolith on Triton will be assisted by conduction by the N_2 atmosphere in the pores. Mendis and Brin (1977) give an expression (their Eq. (15)) for gaseous heat transport by Knudsen diffusion (mean free path > pore diameter) in a porous regolith. Gas conductivity is proportional to mean regolith pore diameter, which is of course unknown, but assuming N_2 gas in vapor pressure equilibrium at 37.5 K, gas conductivity will dominate over grain-contact conductivity if regolith pores exceed 0.1 mm in diameter. The atmosphere may thus also contribute to increasing Triton's regolith conductivity and thermal inertia above the Rhea value.

In conclusion, we adopt the Rhea value of 3×10^4 erg cm^{-2} sec$^{-1/2}$ K^{-1} as a lower limit to the thermal inertia of Triton's surface layers, but expect that the actual value may be much higher.

The thickness of any regolith on Triton is unknown. One constraint is the observed impact crater density, which allows estimation of the thickness of an impact-generated regolith. Strom *et al.* (1990) showed from the few impact craters visible on the Voyager images that Triton's impact crater density is spatially variable and is less than or equal to that of the lunar maria, which have a regolith thickness of ~3–16 m (Quaide and Oberbeck 1968). The likely thickness of an impact regolith on Triton is thus between zero and several meters.

III.B. Seasonal and Permanent Frost

As shown by Spencer (1990) and confirmed by the present work, seasonal N_2 frost deposits on Triton have surface densities up to about 100 g cm^{-2}, or 1 m if the frost is nonporous. Table I shows that the seasonal skindepth in solid N_2 is a factor of 10 greater than this, indicating that the seasonal thermal wave will mostly "see through" the seasonal N_2 deposits. The conductivity of porous N_2 frost will be greater than that for solid frost, because of

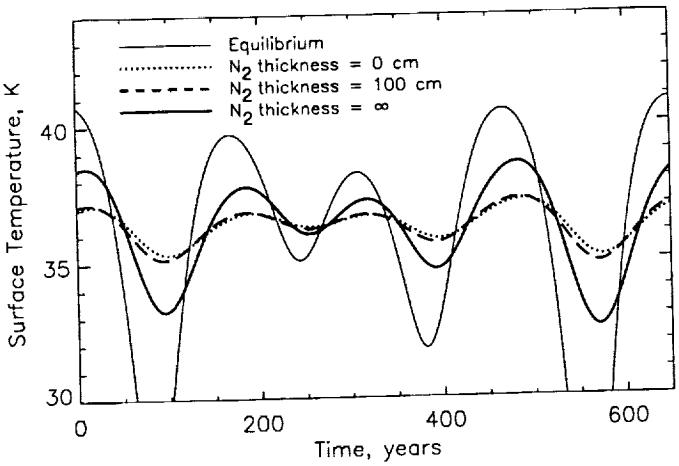

FIG. 1. Demonstration that the heat capacity and conductivity of seasonal N_2 frost has little effect on surface temperatures on Triton. Model surface temperatures at 30° N through a range of Triton seasons are shown for a model consisting of nonporous H_2O overlain by no N_2, 100 cm of N_2, and an infinite thickness of N_2. Equilibrium temperatures, appropriate for a surface with zero thermal inertia, are also shown. N_2 sublimation and deposition are switched off in this model so that the thermal effects of subsurface heat flow can be isolated. One hundred centimeters of N_2, about the maximum thickness of Triton seasonal frost, has very little effect on surface temperatures.

extremely efficient latent heat transfer by N_2 sublimation and deposition across the pores, so that the insulating effects of porous seasonal frost will be even smaller than those of nonporous frost.

The kinetic heat content of the seasonal frost (as opposed to its latent heat content, which is already included in the thermal model) is also negligible. The time required to change the temperature of a frost layer with surface density ρ_S by ΔT, for instance by radiation of heat to space, is of order $(\Delta T \rho_S c)/(\varepsilon\sigma T^4)$. For ρ_S = 100 g cm^{-2}, T = 37 K, the frost can cool by ΔT = 1 K in approximately 3×10^6 sec, or 30 days. This timescale is so short compared to the seasonal timescale that the heat capacity of the seasonal frost can also be ignored.

The seasonal model thus ignores the thermophysical effects of the seasonal frost deposits and calculates surface temperatures as though the seasonal frost were not there, except that it includes the very important effects of the frost latent heat of sublimation. Figure 1 provides more direct justification for this assumption by showing that a 1-m overlying layer of material with the properties of solid N_2 has little effect on the seasonal temperature variations of nonporous H_2O on Triton.

In regions that are permanently frost covered, where the depth of the N_2 deposits is arbitrarily large, the thermal inertia of the surface is assumed to be 5×10^5 erg cm^{-2} sec$^{-1/2}$ K^{-1}, the value for nonporous N_2 (Table I).

IV. OTHER PROCESSES

Another potentially important influence on the N_2 surface temperatures is the α/β phase transition, which occurs at a transition temperature, T_p, of 35 K. To investigate its effects we ran several single-latitude thermophysical models, ignoring the thermal effects of frost sublimation but including the phase transition. The phase transition was incorporated into a standard numerical thermophysical model (Spencer *et al.* 1989) by replacing the thermal energy per unit mass of each subsurface slab, $E_T = cT$, by the total energy per unit mass $E = E_T + H_\beta f_\beta$, where H_β is the latent heat of the phase transition (Table I), and f_β is the β phase mass fraction. For $E < cT_p$, $T = E/c$ and $f_\beta = 0$; for $E > cT_p + H_\beta$, $T = (E - H_\beta)/c$ and $f_\beta = 1$; and for intermediate values of E, where the phase transition is in progress, $T = T_p$ and $f_\beta = (E - cT_p)/H_\beta$.

Figure 2 shows the results of two representative runs. The thermal effect of the phase transition is most pronounced when the mean temperature is near T_p, and the conductivity is high so that the thermal wave propagates deeply and a large volume of N_2 is involved in the transition. The phase transition, as expected, moderates the seasonal temperature variations because energy goes into changing the N_2 phase rather than changing its temperature. The phase change clearly has a significant influence on surface temperatures in some situations, but because of the added computational burden, and because its effects are smaller than those of unknown factors such as the thermal inertia, we did not incorporate the phase transition into our global seasonal thermal model.

The results presented here also do not include the effects of geothermal heat flow from Triton's interior, which has a significant effect on surface temperatures (Brown and Kirk 1991). We have included geothermal heat in several test runs by increasing the temperature at the base of the model at each latitude so that each latitude has a net seasonally averaged heat loss of 6 erg cm^{-2} sec$^{-1/2}$, a reasonable value for Triton's geothermal flux (Hansen and Paige 1992). Geothermal heat increases the temperature of unit-emissivity surfaces by about 0.5 K, and the temperature increase should be inversely proportional to the emissivity. Because the effective albedos in the models presented here (Table II) have been adjusted to yield frost temperatures roughly consistent with the Voyager atmospheric pressure, the main effect of including geothermal heat in the model would be to increase the effective albedos slightly, to counteract the expected 0.5–1.0 K surface temperature increase generated by the geothermal heat.

We also do not consider the heating of the atmosphere by passage over warm frost-free regions (Stansberry *et al.* 1992). To first order, this will not affect frost migration

TABLE II
Parameters of Models Shown in the Figures

Model	Lower layer Γ (erg cm^{-2} sec$^{-1/2}$ K^{-1})	Top layer Γ (erg cm^{-2} sec$^{-1/2}$ K^{-1})	Top layer Heat capacity C (erg cm^{-2} K^{-1})	Top layer Thickness (cm)	Effective albedo A' Frost	Effective albedo A' North hem.	Effective albedo A' South hem.	Run length (years)	1990 atmos. pressure (μbars)	Latitude 1990 cap boundaries N	Latitude 1990 cap boundaries S
A	3×10^4	—	—	—	0.65	0.50	0.50	20,000	13.2	12.5	−42.5
B	1×10^5	—	—	—	0.65	0.50	0.50	20,000	13.4	17.5	−47.5
C	3×10^5	—	—	—	0.65	0.50	0.50	20,000	12.9	27.5	−57.5
D	6×10^5	—	—	—	0.65	0.50	0.50	20,000	14.1	42.5	−67.5
E	1×10^6	—	—	—	0.65	0.50	0.50	20,000	16.8	57.5	−72.5
F	2×10^6	—	—	—	0.65	0.50	0.50	20,000	24.3	67.5	−72.5
G	2×10^6	1×10^5	1×10^9	670	0.63	0.50	0.50	10,000	11.7	27.5	−62.5
H	2×10^6	1×10^5	3×10^8	200	0.63	0.50	0.50	10,000	17.4	42.5	−67.5
I	2×10^6	3×10^4	1×10^9	670	0.63	0.50	0.50	10,000	16.9	12.5	−47.5
J	2×10^6	3×10^4	3×10^8	200	0.63	0.50	0.50	10,000	15.5	12.5	−47.5
K	2×10^6	3×10^4	1×10^8	67	0.63	0.50	0.50	10,000	13.1	22.5	−57.5
L[a]	2×10^6	—	—	—	0.75	0.50	0.50	10,000	15.5	77.5	−27.5
M[a]	2×10^6	—	—	—	0.75	0.40	0.40	10,000	15.7	—	−27.5
N[a]	1×10^6	—	—	—	0.75	0.30	0.30	10,000	15.5	82.5	−27.5
O[a]	2×10^6	—	—	—	0.70	0.50	0.70	40,000	14.8	77.5	−52.5

Note. Models with no top-layer parameters are homogeneous with depth. Top layer thickness was determined from C on the assumption that $\rho = 0.5$ g cm^{-3} and $c = 3 \times 10^6$ erg g^{-1} K^{-1}. Latitude resolution is 5°: cap boundaries are thus multiples of 2.5°.

[a] All frost is in the southern hemisphere at start of run, and the southern cap boundary is maintained at 27.5° S except in model O. All other models start with uniform-thickness frost caps extending from both poles to ±40° latitude.

because it will increase atmospheric temperature without greatly changing atmospheric density. It is the density that is the dominant control on frost sublimation and deposition rates, because the flux of molecules onto the surface is proportional to $n\sqrt{T}$, where n is the number density. The dependence on temperature T is less important because fractional variations in temperature T are much smaller than fractional variations in n, due to the strong dependence of vapor pressure on temperature.

V. MODEL DESCRIPTION

The numerical model is based on that described in Spencer (1990) but includes several extra features. Most importantly, subsurface heat conduction is added to the calculation of surface temperatures. Triton's surface is divided into latitude bands, usually with 5° resolution, and for each band temperature is determined as a function of depth and time, and N_2 frost thickness is calculated as a function of time. A similar thermophysical model has been developed by Hansen and Paige (1992), though their model has higher time resolution (including diurnal effects) but shorter duration and uses different ranges of input parameters.

For areas that are frost free, temperature calculation is essentially identical to that in the conventional thermophysical model described in the Appendix of Spencer *et al.* (1989), except that two-layer models are possible, with an upper layer of different thermophysical characteristics from the substrate. In one-layer models the only important thermophysical parameter is the thermal inertia Γ, but in the two-layer models there are three free thermophysical parameters: the thermal inertias of the two layers and the heat capacity per unit area of the upper layer, C, given by $C = c\rho t$, where t is the layer thickness. The upper layer was normally divided into just three slabs in the numerical model: test runs with higher depth resolution had very similar surface temperatures. Thermophysical properties were assumed to be temperature independent.

For frost-covered regions, we assume, as in Spencer (1990), that all frost has the same surface temperature because of efficient transport of latent heat in the atmosphere (Trafton 1984). Frost surface temperature T_F at each timestep was thus calculated for all frost simultaneously by balancing integrated insolation and heat conduction from the subsurface against thermal radiation into space:

$$\int_a k\left(\frac{\partial T}{\partial x}\right)_{x=0} da + \int_a (1 - A)S\, da = a\varepsilon\sigma T_F^4. \qquad (1)$$

Here $\int_a da$ denotes integration with respect to area over the entire frost-covered surface, a is the total frost-

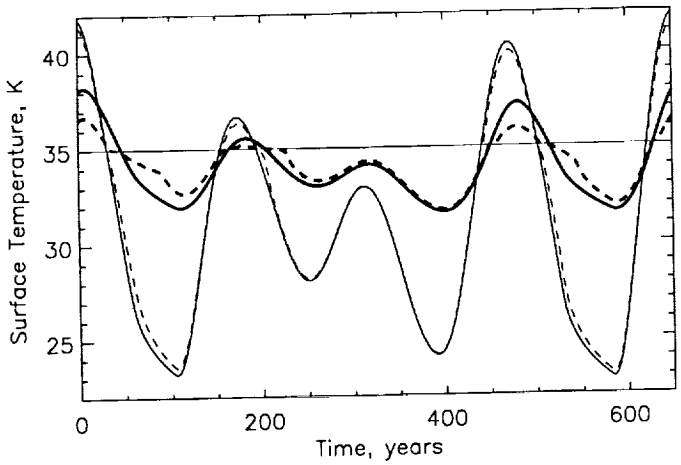

FIG. 2. Effect of the N_2 α/β phase transition on surface temperatures. All models are at 60° N, and as in Fig. 1, the thermal effects of N_2 sublimation and deposition are switched off. The solid lines show surface temperatures in the absence of the α/β phase transition, while dashed lines include the effect of the transition, which occurs at 35 K (horizontal line). Thermal inertias are 1×10^5 (thin lines) and 1×10^6 (thick lines) erg cm^{-2} $sec^{-1/2}$ K^{-1}. The phase transition has more effect for higher thermal inertias because the thermal wave is deeper.

covered surface area, x is the depth into the subsurface, T is the temperature, which is a function of latitude, time, and depth x, A is the bolometric albedo, S is the local insolation, and ε is the emissivity.

We then calculate subsurface temperatures in the frosted regions using the same standard thermophysical model as that in the frost-free regions. We determined the local frost sublimation or deposition rate using the *local* balance between insolation, conduction, radiation, and latent heat transfer,

$$k\left(\frac{\partial T}{\partial x}\right)_{x=0} + (1 - A)S + L\dot{m} = \varepsilon\sigma T_F^4, \qquad (2)$$

where L is the latent heat of sublimation of N_2 frost and $\dot{m}$ is the local rate of frost deposition.

Differing albedos for the frosted and frost-free regions can be specified. Because the emissivities of the surface materials are unknown we used the "effective albedo" A', given by $(1 - A') = (1 - A)/\varepsilon$, as in Spencer (1990), as a measure of the albedo. Equation (2) now becomes

$$k'\left(\frac{\partial T}{\partial x}\right)_{x=0} + (1 - A')S + L\dot{m}' = \sigma T_F^4. \qquad (3)$$

where $k' = k/\varepsilon$ and $\dot{m}' = \dot{m}/\varepsilon$. Actual thermal conductivities and frost thicknesses are thus smaller than the model values k' and m' by the factor ε.

As in the model of Spencer (1990), calculation of temperatures and frost deposition and sublimation rates is continued for long periods (up to 40,000 years) with various initial frost distributions. If sustained sublimation reduces the local frost thickness to zero, that latitude is considered frost-free and the surface temperature is then calculated using the standard thermophysical model. Conversely, if the temperature of a frost-free latitude drops below the current atmospheric temperature, then frost deposition starts at that latitude, and its temperature is determined by Eq. (1). Because the temperature of the lowest slab of the thermal model (which is held constant during each run) has a significant effect on the surface temperatures and frost distribution, this was adjusted iteratively with multiple runs of the model (typically five runs). The base temperature at each latitude was set equal to the seasonally averaged surface temperature at that latitude in the previous run. The globally and seasonally averaged thermal balance of the model (ratio of total insolation to total thermal emission) improved with each run and by the final run mean insolation and emission were typically balanced to better than 1 part in 10^4. Our 1990 model showed that a global average of no more than about 20 g cm^{-2} of N_2 frost migrated seasonally, so the present model used a global frost inventory of 50 g cm^{-2} to ensure full development of seasonal frosts. Excess frost collects at the poles.

An additional option was added to the model in response to the suggestion of Brown and Kirk (1991) and Kirk and Brown (1991) that the secular migration of volatiles to Triton's poles, mentioned in Section I.A, might be balanced by viscous spreading of the permanent polar caps toward lower latitudes. We simulated such a cap, when desired, by defining the cap to be the region poleward of a specified latitude and redistributing the frost deposits in the cap region as necessary to prevent bare ground from being exposed within the cap boundary. The redistribution conserved the total frost inventory within the cap boundary, which could however change due to normal sublimation processes.

VI. MODEL RESULTS

VI.A. Hemispherically Symmetric Models

A primary motivation for the thermal modeling was to investigate the possibility that frost deposition in the darker northern hemisphere seen by Voyager might be inhibited by the finite thermal inertia of the subsurface, i.e., that the visible regions had not yet cooled off enough from the previous northern summer to develop thick frost deposits. Figure 3 and 4a show results for various substrate thermal inertias, assuming substrate thermal properties constant with depth. Values of $\Gamma > 5 \times 10^5$ erg cm^{-2} $sec^{-1/2}$ K^{-1}, well within the range of plausible thermal inertias for Triton, are sufficient to prevent deposition

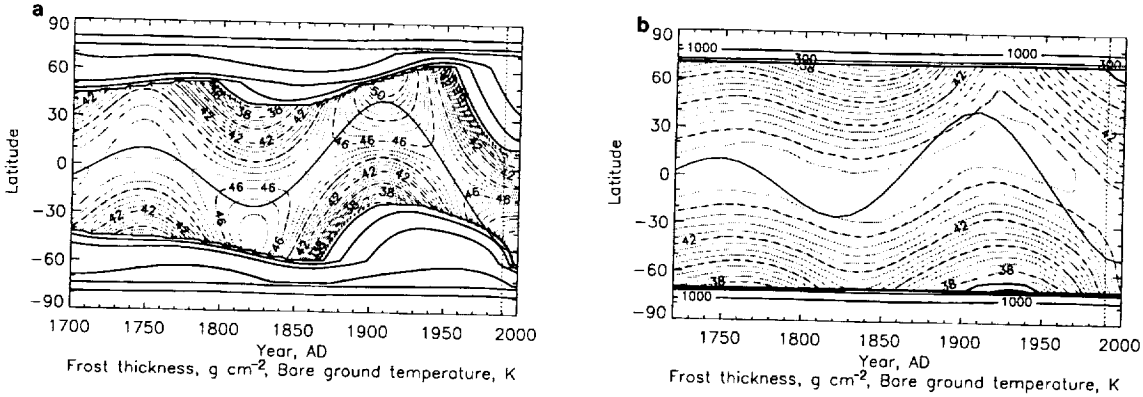

FIG. 3. Frost thickness (bold contours) and bare ground temperatures (dashed contours) vs time and latitude for two extreme substrate thermal inertias (Γ): 3×10^4 (a; model A in Table II) and 2×10^6 erg cm^{-2} sec$^{-1/2}$ K^{-1} (b; model F in Table II). Frost thickness contours are at 1, 3, 10, 30, 100, 300, and 1000 g cm^{-2}. a is very similar to models where $\Gamma = 0$ is assumed, e.g., Fig. 1. of Spencer (1990), with extensive northern seasonal frosts at the time of the Voyager encounter (dotted vertical line). In b, in contrast, the high thermal inertia suppresses almost all seasonal frost and reduces seasonal temperature variations in the frost-free regions. The curve oscillating about the equator marks the locus of the subsolar point.

of fresh frost in the northernmost regions visible to Voyager at the time of the encounter. Because porosity in nonvolatile substrates will reduce Γ, the thermal inertia of a CH_4 substrate could prevent visible northern frost only if it was effectively nonporous (Eluszkiewicz, personal communication), but somewhat porous H_2O and CO_2 substrates are consistent with the lack of visible northern frost (Table I). These runs require an effective bolometric frost albedo of 0.65 to maintain the observed atmospheric pressure, lower than photometric estimates of Triton's southern hemisphere albedo. The discrepancy, similar to that found in the simpler models of Spencer (1990) and Stansberry *et al.* (1990), may indicate a low emissivity for the N_2 frost on Triton. Including geothermal heat in the model would reduce the discrepancy and increase the inferred emissivity slightly (Section IV).

Figure 4b shows a similar plot for two-layer thermophysical models, in which a lower semi-infinite layer $\Gamma = 2 \times 10^6$ erg cm^{-2} sec$^{-1/2}$ K^{-1}, appropriate for nonporous H_2O or CO_2, is covered with a variable-thickness "regolith" of Rhea-like material ($\Gamma = 3 \times 10^4$) or a more conductive regolith ($\Gamma = 1 \times 10^5$). Again, as expected, a thinner regolith inhibits frost formation in the northern hemisphere at the time of the Voyager encounter. Model H, with 2 m of regolith that has three times the thermal inertia of Rhea, overlying nonporous H_2O or CO_2 ice, a very plausible thermophysical structure based on the arguments of Section III.A, is frost-free in the northern hemisphere as far north as Voyager could see. An effective albedo of 0.63 is used for the two-layer model to achieve rough consistency with the observed atmospheric pressure, again suggesting a low emissivity for the N_2 frost.

All these models suffer from the problem of ever-shrinking permanent polar caps, first encountered by Spencer (1990) and Stansberry *et al.* (1990). They predict that most

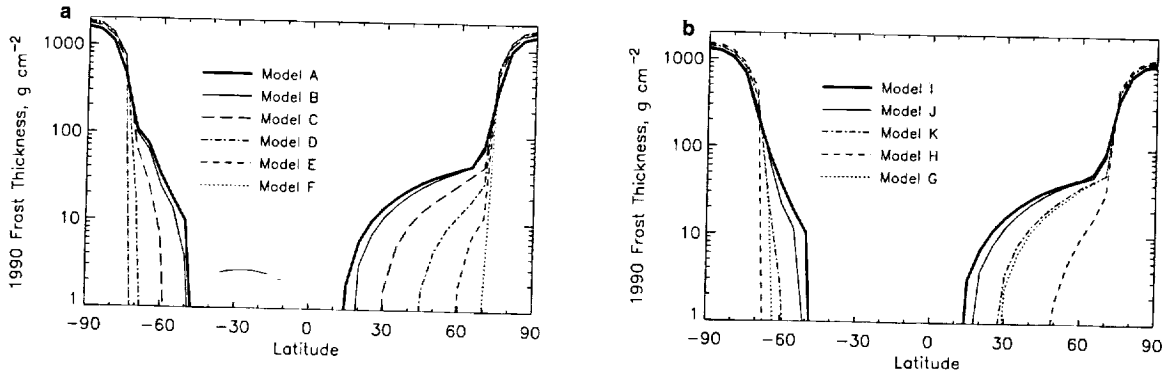

FIG. 4. Frost thickness vs latitude at Voyager encounter time for various thermal models. a shows results of homogeneous substrate models A–F. Low-latitude frost thickness decreases monotonically with increasing Γ, though in the southern hemisphere models E and F coincide. b shows results of two-layer models with substrate Γ consistent with nonporous H_2O or CO_2.

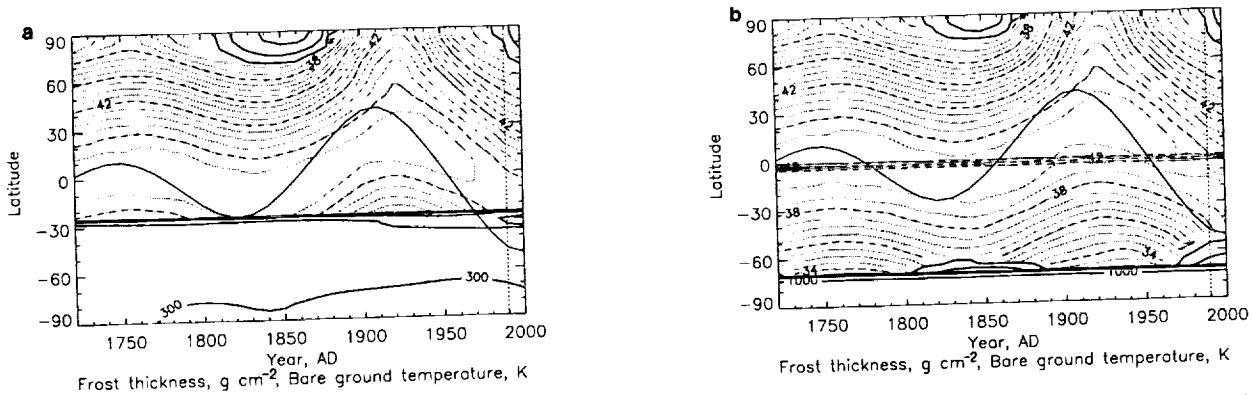

FIG. 5. Like Fig. 3, but for models with permanent hemispheric asymmetry. a shows model L: the boundary of the southern cap is maintained artificially at 27.5° S (see text). Note the presence of a temporary northern winter frost cap in this particular model. b shows model O, in which the southern cap is allowed to shrink but the southern hemisphere substrate is brighter than in the northern hemisphere. Note the appearance of southern hemisphere frosts *in summer*.

of Triton's N_2 inventory will retreat to the poles, and the southern hemisphere at the time of the Voyager encounter should have been mostly frost-free, with a residual seasonal cap extending no further north than about 45° S.

VI.B. Koyaanismuuyaw Models

If all the frost is initially placed in the one hemisphere (the southern one, for instance), and the substrate material has sufficiently low albedo and high thermal inertia, then the exposed substrate of the northern hemisphere never cools off enough in the winter to allow a permanent cap to form there. However, the southern cap still shrinks monotonically with time and eventually all but the extreme southern latitudes of Triton are frost-free. If, however, the permanent polar cap is forced to maintain a large size, as by viscous spreading or any other process, it is possible to maintain a frost-covered southern hemisphere and frost-free northern hemisphere indefinitely under some circumstances, as suggested in the Koyaanismuuyaw hypothesis of Moore and Spencer (1990). Figure 5a shows an example of this (model L).

Figure 5b shows a rather different model, model O, in which the southern cap is not forced to maintain a fixed size but the substrate in the southern hemisphere of Triton is as bright as the frost ($A' = 0.70$). The northern hemisphere substrate has $A' = 0.50$. Winter seasonal frosts form in the northern hemisphere, as in model L, but, paradoxically, *summer* seasonal frosts form in the south. This is because in this model the permanent cap Γ is less than the substrate Γ [as is reasonable if the cap is nonporous N_2 and the substrate is nonporous H_2O or CO_2 (Table I)], so during the southern summer the frost temperature increases faster than the temperature of the bright southern hemisphere substrate. When the frost temperature exceeds the nearby substrate temperature, summer frost forms. This model reflects the idea, suggested by Moore and Spencer (1990) and discussed in Section VII.B, that the nonvolatile material in the southern hemisphere may be intrinsically bright.

If even a small permanent cap forms in the northern hemisphere and has the same albedo as the southern cap, the southern cap becomes unstable with respect to the north cap because it extends to lower latitudes and thus has greater mean seasonally averaged insolation. Frost then rapidly transfers to the northern hemisphere until the southern cap shrinks to the size of the northern cap. This severely limits the range of conditions under which the global asymmetry can be maintained, and the allowed range is shown in Fig. 6 for the case of a homogeneous (one-layer) substrate. The models shown in Fig. 6 all have an effective frost albedo of 0.75, which results in an atmospheric pressure consistent with the Voyager observations when the models are stable. Note that the observed atmospheric pressure is achieved with an effective frost albedo higher (and thus a higher emissivity) than that in the hemispherically symmetric case. This is because the lack of a large northern polar cap in the Koyaanismuuyaw models increases the global mean insolation on the frost in 1989, and this increases the frost temperature for a given albedo. Figure 6 shows that unless the Triton's north polar regions are much darker than the regions seen by Voyager or have very low emissivity, a global frost asymmetry can only be maintained if, as is certainly possible, the thermal inertia of the substrate is very close to that for H_2O or CO_2 ice.

Koyaanismuuyaw models with a two-layer substrate in which the upper "regolith" layer is thin enough to maintain the global frost asymmetry are time-consuming to calculate because extremely high time resolution is required to maintain numerical stability. For this reason, we have not yet explored such models in detail.

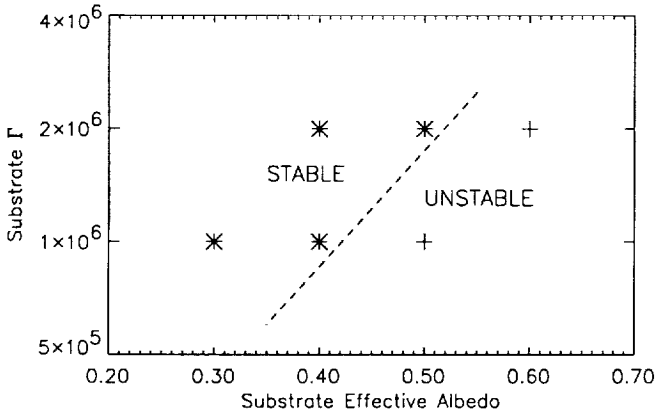

FIG. 6. The values of effective substrate albedo and thermal inertia (in units of erg cm^{-2} $sec^{-1/2}$ K^{-1}) for which a hemispheric asymmetry in frost distribution is stable on Triton. Frost is initially confined to one hemisphere, and "*" indicates model runs in which all the frost remains in its initial hemisphere. "+" indicates runs in which a permanent polar cap forms in the initially frost-free hemisphere and destroys the global asymmetry. The approximate boundary between the two regimes is shown. The frost effective albedo is 0.75 in all models and is constrained by the N_2 atmospheric pressure observed by Voyager.

VI.C. Atmospheric Stability

Atmospheric pressure as a function of time is obtained from the frost temperature and the N_2 vapor pressure curve (Brown and Ziegler 1980). The timescale t_a for changing the atmospheric pressure is given by the ratio of its latent heat content to the rate of radiative heat loss; i.e., $t_a = Lm_a/(\varepsilon\sigma T^4)$, where m_a is the column density of the atmosphere (Trafton and Stern 1983). For an N_2 atmosphere at 38 K and an emissivity of 0.7, t_a = 86 days, which is much shorter than the seasonal timescale. We have already shown that the specific heat of the seasonal frost deposits is not a significant factor in moderating surface temperature changes (Fig. 1 and Section III.B). We thus assume that the atmospheric pressure adjusts instantaneously to changes in frost temperature.

The frost migration models of Spencer (1990), which assumed a surface with zero thermal inertia, predicted a very unstable atmospheric pressure and a possible atmospheric collapse within the next decade as the remains of the previous winter's seasonal cap sublimated away during the southern summer. Including a finite thermal inertia moderates these changes somewhat and may even result in a pressure *increase* in the coming decade, but large atmospheric pressure variations still occur, as shown in Fig. 7.

High-thermal-inertia substrate models have increasing atmospheric pressure at present because insolation is increasing on the southern cap and there is little northern seasonal frost to radiate the heat away (remember that frost temperature is determined by the mean insolation on all surface frosts). Low-thermal-inertia substrate models, with extensive seasonal frost deposits, have currently decreasing atmospheric pressure because of the decreasing area of sunlit southern seasonal frost and the large area of shadowed northern seasonal frost. Koyaanismuuyaw models, with no permanent northern cap at all, show the most extreme pressure variations because during northern summer almost all the surface N_2 frost is in darkness. Triton's atmospheric pressure can occasionally be monitored from Earth by means of stellar occultations, so there is a chance to distinguish observationally between these models in years to come.

As in Spencer (1990), the model implicitly assumes that the atmospheric pressure is always above about 1 μbar. At lower pressures winds due to volatile migration become supersonic and the condition of isothermality inherent in the model ceases to apply. However, the only models with extensive periods of submicrobar atmospheric pressure are the Koyaanismuuyaw ones, and in these there is negligible frost migration anyway, so the low pressures do not invalidate these models.

VII. DISCUSSION

VII.A. Northern Hemisphere

We have demonstrated that seasonal subsurface heat storage, with reasonable assumptions about surface structure, can prevent or greatly reduce frost deposition in visible northern latitudes at the time of the Voyager encounter and thus provides a plausible explanation for the relative darkness of this part of Triton. Recent work by Lee *et al.* (1992) has shown that the dark regions of the northern hemisphere are anomalously forward-scattering, which may indicate the presence of a thin, relatively transparent layer of fresh frost, and Eluszkiewicz (1991) has shown how such a layer might form in N_2 frost. The equilibrium model of Spencer (1990) predicted 20–30 g cm^{-2} of N_2 frost in this region, but the current model allows much thinner frost deposits in the visible northern hemisphere, which might be more easily made transparent. However, if the anomalously scattering region is indeed covered by a transparent frost layer, the thermal inertia in this region must be small enough to allow at least some frost deposition.

Yelle (1992) suggested another explanation for the relative darkness of Triton's northern hemisphere: that frost is deposited preferentially in colder shaded regions where it is less visible. This mechanism could work in conjunction with the finite thermal inertia to reduce the visibility of frost deposits in this region.

The suggestion of Spencer (1990) that fresh N_2 frost on Triton might be relatively dark is not directly addressed by the new models. This remains a possible explanation

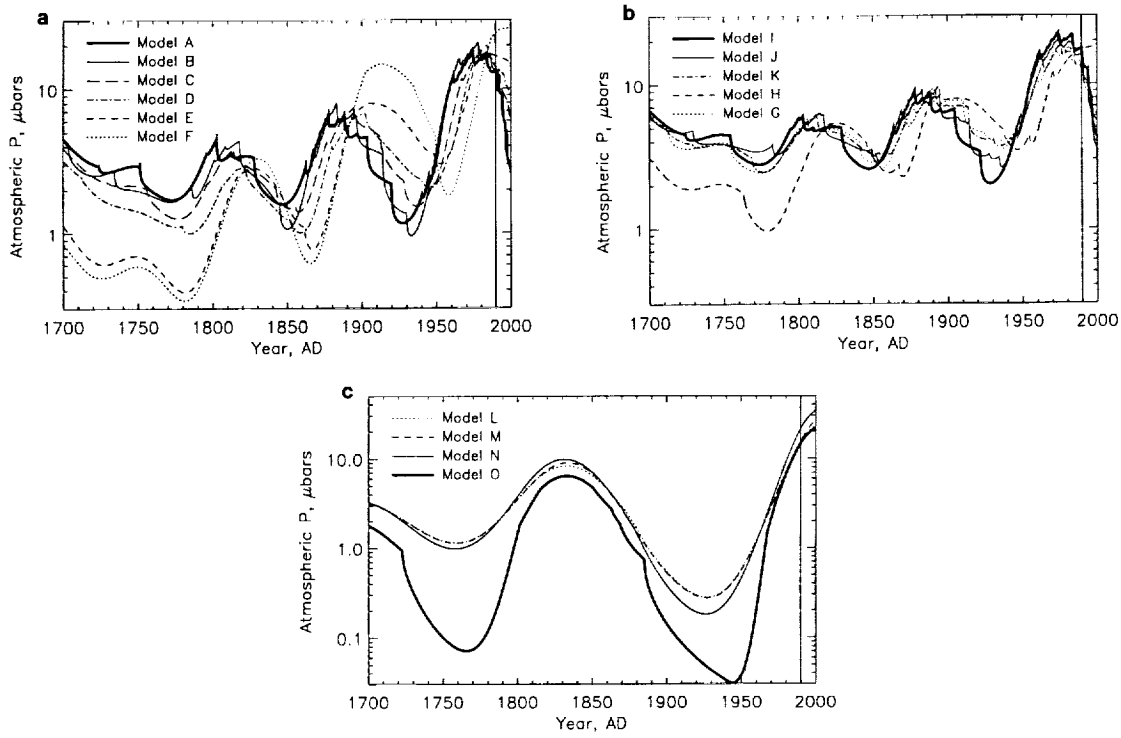

FIG. 7. History of atmospheric pressure for various models. The time of the Voyager encounter is shown by a vertical line. a shows homogeneous substrate models, b shows two-layer substrate models, and c shows "Koyaanismuuyaw" models, with all permanent frost in the southern hemisphere. The scalloping of the curves is an artifact caused by the finite latitude resolution and consequent sudden changes in surface frost coverage, but higher-resolution runs show the same average behavior. Atmospheric pressures of less than about 1 μbar violate the condition of frost isothermality assumed by the model.

for the darker northern hemisphere, in addition to the possibilities mentioned above.

VII.B. Southern Hemisphere

We have not solved the problem of the apparent large extent of the bright material in the southern hemisphere *if* this material is predominantly N_2, because secular poleward migration of the permanent polar caps occurs in the thermophysical models as in earlier equilibrium models, and seasonal frosts are not very extensive in the southern hemisphere at the time of the Voyager encounter in any of our models. The viscous spreading model of Brown and Kirk (1991) and Kirk and Brown (1991) provides a mechanism for maintaining a large southern cap of bright N_2, but only if all permanent low-latitude N_2 deposits are physically connected by flowing "glaciers" to deposits at much higher latitudes. The presence of isolated low-latitude high-albedo patches, such as the aureoles of the "mushrooms" at approx. 20° S, 60° E (Fig. 30 of Smith *et al.*, (1989)), is difficult to explain by this mechanism, and if this bright material is not N_2 it is plausible that much of the rest of the bright material in the contiguous bright regions is not N_2 either. Also, the visibility of the global linear ridge network in the extreme southern latitudes implies that any frost deposit is probably less than 1 km thick.

Recent spectroscopic observations by Cruikshank *et al.* (1991 and personal communications) show the presence of CO_2 on Triton's surface. The depth of the deepest CO_2 features is about 10%, comparable to the depth of CO_2 absorptions on the Martian CO_2 polar cap. The minimum areal coverage of CO_2-containing material on Triton, if the intrinsic depth of the bands in pure CO_2 was 100%, is thus 10% of the projected disk (weighted by the continuum albedo at 2 μm). However, if the Martian cap spectrum is a good analog, the intrinsic depth of the CO_2 features may be much less than 100%, and the areal coverage on Triton correspondingly much greater. Because only 12% of Triton's projected disk was occupied by the northern hemisphere at the time of the observations, it is quite likely that a considerable fraction of the southern hemisphere is occupied by CO_2, a nonvolatile material at Triton temperatures. These observations thus lend support to the idea that at least some of the bright material in the southern hemisphere is nonvolatile substrate rather than N_2 frost. As mentioned by Spencer (1990), the strong CH_4 absorptions in Triton's spectrum (Cruikshank *et al.* 1988,

Spencer *et al.* 1990, Grundy and Fink 1992) also provide evidence for extensive nonvolatile exposure in the southern hemisphere, because although CH_4 is somewhat volatile, its surface abundance is probably greater than its atmospheric abundance. However, if much of the exposed bright southern material is nonvolatile, its high albedo in the presence of possible dark airborne particulates from the plumes (Soderblom *et al.* 1990) may require a cleaning mechanism. Possibilities include the removal of dark particles by wind (Sagan and Chyba 1990), especially during periods of high atmospheric pressure, or endogenic resurfacing.

Yelle (1992) argues that the westward winds at 10 km altitude at 50° S latitude, revealed by the active plumes there, require that the equatorial regions be warm and probably frost-free. However, it is also possible that the warmer frost-free regions are part of the bright southern hemisphere materials: warm frost-free regions anywhere northward of 50° S could explain the wind directions at the latitude of the plumes.

Moore and Spencer (1990) noted that the bright southern hemisphere material has appreciable thickness ($>\sim$10 m) and discrete boundaries and occupies low-lying areas, which is consistent with a material endogenically emplaced. Thus the hemispheric asymmetry of Triton may be analogous to that of Mars, whose northern half has been resurfaced by endogenic materials.

We suggest that these arguments and the model presented here provide additional evidence that much of Triton's bright southern hemisphere is high-albedo nonvolatile material, probably with intermixed permanent and remnant seasonal N_2 frost, as suggested by Spencer (1990). The gross hemispheric albedo asymmetry may be due to the difference in the intrinsic albedos of endogenically emplaced refractory materials composing the substrate and not be dependent on the precipitation of volatiles. Model O (Fig. 5b) shows that summer seasonal frosts may occur if there is high-albedo nonvolatile material in the southern hemisphere. It is even possible that the appearance of a southern hemisphere summer frost, covering previously exposed UV-dark material, contributed to the remarkable apparent increase in Trition's UV albedo and possible decrease in CH_4 absorption strength during the 1980s (Cruikshank *et al.* 1988, Smith *et al.* 1989, McEwen 1990, Pollack *et al.* 1990).

VII.C. Permanent Hemispheric Asymmetries

Models L–O presented here show that it is possible for almost all the N_2 frost to remain permanently in the southern hemisphere, but only if the northern hemisphere has a low effective albedo *and* high thermal inertia. In this case the effective albedo (and thus the emissivity) of the N_2 frost is higher than that in the hemispherically symmetric case, because the frost loses no heat by radiation from the winter hemisphere and can be warmer for a given albedo.

ACKNOWLEDGMENTS

We thank Bob Pappalardo and Steven Croft for their diligent searches for the cryogenic ice thermophysical parameters used in this model and Steven Croft for proofreading Table I. Robert H. Brown, Candy Hansen, David Paige, Randy Kirk, Jim Pollack, Paul Schenk, and Janusz Eluszkiewicz provided stimulating discussions and ideas, and reviews by Roger Yelle and John Hillier helped to improve the paper. The work was supported by NASA Grant NAGW-2742.

REFERENCES

BROADFOOT, A. L., *et al.* 1989. Ultraviolet spectrometer observations of Neptune and Triton. *Science* **246,** 1459–1466.

BROWN, G. N., AND W. T. ZEIGLER 1980. Vapor pressure and heats of vaporization and sublimation of liquids and solids of interest in cryogenics below 1-atm pressure. *Adv. Cryo. Eng.* **25,** 662–670.

BROWN, R. H., AND R. L. KIRK 1991. Coupling of internal heat to volatile transport on Triton. *Bull. Am. Astron. Soc.* **23,** 1210.

CRUIKSHANK, D. P., R. H. BROWN, A. T. TOKUNAGA, R. G. SMITH, AND J. R. PISCITELLI 1988. Volatiles on Triton: The infrared spectral evidence 2.0–2.5 μm. *Icarus* **74,** 413–423.

CRUIKSHANK, D. P., T. C. OWEN, T. R. GEBALLE, B. SCHMITT, C. DEBERGH, J-P. MAILLARD, B. L. LUTZ, AND R. H. BROWN 1991. Tentative detection of CO and CO_2 ices on Triton. *Bull. Am Astron. Soc.* **23,** 1208.

ELUSZKIEWICZ, J. 1991. On the microphysical state of the surface of Triton *J. Geophys. Res.* **96,** 19217–19230.

GRUNDY, W. M., AND U. FINK 1992. Constraints on the grain size and mixing ratio of CH_4 and N_2 ice aggregates on Triton's surface. In *Proc. Neptune and Triton Conference, Tucson, AZ,* abstract volume, p. 27.

HANSEN, C. J., AND D. A. PAIGE 1992. A thermal model for the seasonal nitrogen cycle on Triton. *Icarus* **99.**

HILLIER, J., P. HELFENSTEIN, A. VERBISCER, AND J. VEVERKA 1991. Voyager photometry of Triton: Haze and surface photometric properties *J. Geophys. Res.* **96,** 19203–19209.

INGERSOLL, A. P. 1990. Dynamics of Triton's atmosphere. *Nature* **344,** 315–316.

KIRK, R. L., AND R. H. BROWN 1991. Models for the viscous spreading of Triton's permanent polar caps *Bull. Am. Astron. Soc.* **23,** 1209.

LEE, P., P. HELFENSTEIN, J. VEVERKA, AND D. MCCARTHY 1992. Anomalous scattering region on Triton. *Icarus,* in press.

MCEWEN, A. S. 1990. Global color and albedo variations on Triton. *Geophys. Res. Lett.* **17,** 1765–1768.

MENDIS, D. A., AND G. D. BRIN 1977. Monochromatic brightness variations in comets. *Moon* **17,** 359–372.

MOORE, J. M., AND J. R. SPENCER 1990. Koyaanismuuyaw: The hypothesis of a perennially dichotomous Triton. *Geophys. Res. Lett.* **17,** 1757–1760.

POLLACK, J. B., J. M. SCHWARTZ, AND K. RAGES 1990. Scatterers in Triton's atmosphere: Implications for the seasonal volatile cycle. *Science* **250,** 440–443.

QUAIDE, W. L., AND V. R. OBERBECK 1968. Thickness determination of the lunar surface layer from lunar impact craters. *J. Geophys. Res.* **73,** 5247–5270.

SAGAN, C., AND C. CHYBA 1990. Triton's streaks as windblown dust. *Nature* **346,** 546–548.

SMITH, B. A., L. A. SODERBLOM, *et al.* 1989. Voyager 2 at Neptune: Imaging science results. *Science* **246,** 1422–1449.

SODERBLOM, L. A., S. W. KIEFFER, T. L. BECKER, R. H. BROWN, A. F. COOK, C. J. HANSEN, T. V. JOHNSON, R. L. KIRK, AND E. M. SHOEMAKER 1990. Triton's geyser-like plumes: Discovery and basic characterization. *Science* **250,** 410–415.

SPENCER, J. R. 1988. The thermal inertias and albedos of Rhea and Tethys. *Bull. Am. Astron. Soc.* **20,** 854. [Abstract]

SPENCER, J. R. 1989. The thermal inertias of Rhea, Dione, and Tethys from ground-based radiometry. *Bull. Am. Astron. Soc.* **21,** 983. [Abstract]

SPENCER, J. R. 1990. Nitrogen frost migration on Triton: A historical model. *Geophys. Res. Lett.* **17,** 1769–1772.

SPENCER, J. R., M. W. BUIE, AND G. L. BJORAKER 1990. Solid methane on Triton and Pluto: 3- to 4-μm spectrophotometry. *Icarus* **88,** 491–496.

SPENCER, J. R., L. A. LEBOFSKY, AND M. V. SYKES 1989. Systematic biases in radiometric diameter determinations. *Icarus* **78,** 337–354.

STANSBERRY, J. A., J. I. LUNINE, C. C. PORCO, AND A. S. MCEWEN 1990. Zonally averaged thermal balance and stability models for Triton's polar caps. *Geophys. Res. Lett.* **17,** 1773–1776.

STANSBERRY, J. A., R. V. YELLE, AND J. I. LUNINE 1992. Energy coupling between Triton's surface and atmosphere. *Icarus* **99.**

STROM, R. G., S. K. CROFT, AND J. M. BOYCE 1990. The impact cratering record on Triton. *Science* **250,** 437–439.

SYKES, M. V., R. M. CUTRI, L. A. LEBOFSKY, AND R. P. BINZEL 1987. IRAS serendipitous survey observations of Pluto and Charon. *Science* **237,** 1336–1340.

TRAFTON, L. 1984. Large seasonal variations in Triton's atmosphere. *Icarus* **58,** 312–324.

TRAFTON, L., AND STERN, S. A. 1983. On the global distribution of Pluto's atmosphere. *Astrophy. J.* **267,** 872–881.

YELLE, R. V. 1992. The effect of surface roughness on Triton's volatile distribution. *Science* **255,** 1553–1555.